

Automatic Classification of Olive Leaves Disease Based on Adaptive Neuro-Fuzzy Inference System with Hybrid Features

Iman Hussein AL-Qinani

Department of Computer Science, College of Education, Mustansiriyah University, Baghdad, Iraq

ARTICLE INFO

Article History:

Accepted : 24 Jan 2025

Published: 27 Jan 2025

Publication Issue :

Volume 12, Issue 1

January-February-2025

Page Number :

136-147

ABSTRACT

Modern economies in many nations owe a great deal to the production of crops. Foliar diseases may cause immense damage to many different types of crops. These crops include wheat, olive, fruit, and many more. New AI breakthroughs require more precise identification of olive leaf diseases. An adaptive neuro-fuzzy inference system (ANFIS) is suggested based on mixed features to determine whether olive leaves are healthy or infected. Images of olive leaves are processed in various ways to enhance them, such as increasing contrast and filtering to remove unwanted noise. Olive leaf segmentation is performed using the k-means method. Several methods are combined to create hybrid features, including statistical moment invariants, a feature histogram, and a grey-level co-occurrence matrix (GLCM). The obtained characteristics are analyzed in this study to measure their potential discriminative ability between healthy and diseased olive leaves. In conclusion, the proposed approach provides a more accurate and efficient result for categorization. The suggested model achieves a remarkable 98.5% accuracy in its predictions.

Keywords: Classification, Clustering, Hybrid features, Olive, Leaves diseases.

INTRODUCTION

The rapid advancement of AI and ML-based systems has opened up many new domains for computer vision (CV) applications. There are several applications of ML and deep learning (DL) for solving CV problems, for example, Video summarisation [1], speaker identification [2], Wildfire detection [3-4], Temperature prediction [5-6], Spam detection [7], Contextual anomaly detection [8], Sentiment Analysis

[9], Segmentation [10], and Documents image classification [11].

Disease detection strategies based on ML and DL are gaining prominence in AI studies in agriculture. Plants exhibit extreme diversity in species, complexity, and features, so several studies have proposed using AI to analyze these features [12-14]. Farmers have been cultivating olive trees for centuries - rightly so because they are among the best

and brightest in the plant kingdom. Researchers have spent a lot of time trying to figure out what causes olive leaf diseases, but they have had a hard time because symptoms vary from plant to plant and even among leaves of the same plant. Peacock spot disease, aculeus olearius, olive tree knot, and bacterial disease are just a few diseases affecting olive leaves [15]. The productivity of olive trees is highly dependent on the health of the plants, so accurate and timely detection of diseases before harvesting olive leaves is crucial [16-19].

The proposed model enhances the olive leaf image by changing the contrast and removing noise and other unwanted components. Then, the image is segmented to isolate the interesting parts using the k-mean model. Once the leaf detection process is completed for the input image, the third step is to perform classification based on the features obtained by the feature extraction technique. This procedure is applied to the segmented leaves to extract valuable information. In addition, ANFIS was used to classify infected and healthy olive leaves.

Motivation: To reduce agricultural losses, ML is used to provide thorough crop suggestions and insights to farmers. Worldwide, agriculture is responsible for 15.4% of the gross domestic product [20]. More efficient and accurate farming with less human labor is made possible by applying ML in agriculture. One of the essential components of ML is image classification. The biggest challenges in classifying images come from the fact that they are essentially huge matrices with many pixels, which are inherently very complex. ML takes a lot of time and effort to classify images accurately, which is fraught with many difficulties [21]. Accurately recognizing objects in images and adapting to changes in illumination, scale, and orientation are just some of these difficulties. The development of reliable image classification systems requires solving these problems. The following are some of the limitations of current image classification systems: high complexity in space

and time, falling in local optima due to the use of heuristic techniques, and the accuracy and performance of the low predictions [22].

Contribution: (a) The proposed model reduces the limitations of recent methodologies. It uses a consistent combination of image processing methods. (b) The statistical feature extraction technique helps the classifier (ANFIS) to predict with high accuracy, and the model overall has low complexity and high performance.

Paper organization: In total, this work consists of five parts. An introduction (1) and a literature review (2) are given. A detailed explanation of the methodology is provided in (3), and the dataset and results are examined in light of the algorithms from the literature review in section (4). The final section (5) provides some concluding thoughts, and references for those who wish to learn more.

LITERATURE REVIEW

This section presents recent work using ML and DL models to diagnose disease in olive tree leaves. Uğuz et al. [18] applied transfer learning techniques to their proposed CNN in addition to the VGG16 and VGG19 architectures. One of the goals of this study was to investigate how adding more data affects efficiency. It also examined how the Adam algorithm, the AdaGrad method, the Stochastic Gradient Descent algorithm (SGD), and the RMS Prop algorithm affect the network's performance. The experiments showed that the Adam and SGD optimization algorithms generally give better results. Alshammari et al. [19] deep learning (DL) paradigm for olive leaf disease categorization was presented. They achieved this using a modified genetic algorithm and three different DL models (AlexNet, DenseNet, and ResNet). However, the models that used metaheuristic techniques are unstable and may fall into a local optimum. Alshammari et al. [21] devised a novel approach to deep ensemble learning by combining a model of the vision transformer (ViT) and a model of

the convolutional neural networks (CNN). The olive leaves are susceptible to various diseases, and this procedure aims to identify and categorize those diseases. The weakness of the proposed system lies in feature extraction, as the ViT method requires a large amount of data to learn everything from scratch and is, therefore, unsuitable for real-time plant disease detection. Raouhi et al. [23] collected data at various stages of development from several sites in Morocco to create a data set on olive diseases. This model design outperformed eight others standard CNNs in a head-to-head competition. The proposed model suffers from overfitting due to the stacking of the same module, which is highly complex. Sinha et al. [24] developed an objective approach for recognizing olive tree illnesses that cause spots on the leaves. The leaf images of such diseases contain specific parameters and values that aid in determining the disease types.

METHOD

3.1. Proposed methodology and related techniques

The general framework of the proposed model consists of the following steps:

1. Input Image (Leaves Olive image).
2. Image Preprocessing: adjust contrast, and remove noise and undesired components.
3. Image Segmentation: via the k-means algorithm.
4. Feature extraction: first-order statistics (Mean, Variance, Skewness, and Standard Deviation), GLCM (Homogeneity, Entropy, Energy, etc.), and Moment Invariants features.
5. Classification by ANFIS.

3.1.1. Image pre-processing

Using reduced noise and enhancement strategies leads to higher precision in identifying regions of interest in images of olive leaves. To achieve this goal, the median filtering approach is used to clean images, and the contrast is adjusted. For this reason, changing the image intensity values was used. After completing this step, the image is free of distortion. Fig. 1 shows

that the image quality and the contrast have the highest quality.

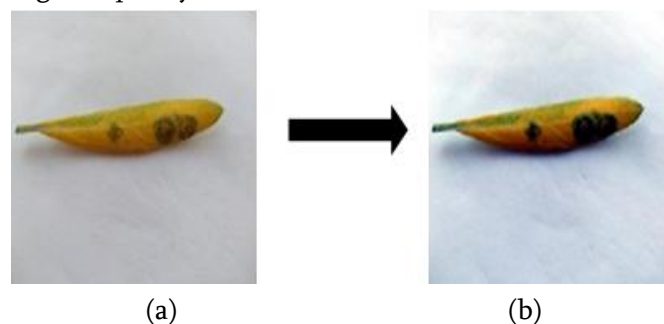


Figure. 1 Pre-processing step: (a) source image and (b) contrast enhancement of image

3.1.2. Segmentation

In the context of image processing, it is partitioning an image into homogeneous regions. Many techniques exist for segmentation, such as the RGB-to-HIS (hue, intensity, and saturation) model conversion, the Otsu approach, UNet, CNN model, the k-means clustering algorithm, etc [25-26].

3.1.2.1. K-Means clustering

An example of an unsupervised iterative technique is K-Means clustering, which divides a dataset into k groups according to their distance from a chosen centroid [27]. In each loop, the centroids are recalculated to account for the most recent data. As a direct consequence of applying the K-Means technique, each data point is either placed in a cluster or left unassigned. The image is first transformed from RGB to $L^*a^*b^*$ model, where "L" is luminosity layer, "a*" and "b*" is chromaticity-layer; all color information is in the "a*" and "b*" layers." Here, the K-means method separated olive leaves from their background. Feature extraction and olive leaf categorization can both benefit from segmentation. Like the clustering process, the k-means method splits a dataset into K groups of independent clusters. The Euclidean distance has utilized a formula for centroid data to determine the separation [28]. Fig. 2 demonstrates that the K-means clustering technique effectively extracted the segments from the image. Once the image has been segmented by K-means clustering, choose a threshold that allows for the least

amount of grayscale to binary transition using Otsu's approach [29].

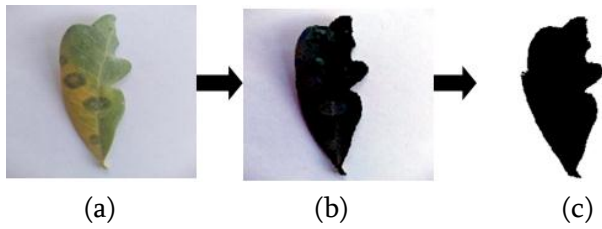


Figure. 2 Segmentation step: (a) source image (b) applying K-means and (c) using 'Otsu's method

3.1.3. Feature extraction

Feature extraction isolates the relevant features, which leads to understanding the leaves' olive diseases images well.

3.1.3.1. Statistical moment invariants

Hu constructed a collection of invariants using algebraic invariants, and he was the first person to do so. The concept of employing moments in shape recognition became widely accepted. The moments in two dimensions of an M-by-M pixel image with "grey function f (x, y) (x, y = 0... M - 1) " are formulated in the form of [30-32]:

$$" m_{pq} = \sum_{x=0}^{M-1} \sum_{y=0}^{M-1} x^p y^q f(x, y) " \tag{1}$$

The definition of a moment f (x, y) in terms of (a, b) is as follows:

$$" \mu_{pq} = \sum_x \sum_y (x + a)^p \cdot (y + b)^q f(x, y) " \tag{2}$$

Thus, the center moments m'_{pq} or μ_{pq} may be calculated from (2) by substituting "a = - \bar{x} and b = - \bar{y} "as,

$$" \bar{x} = \frac{m_{10}}{m_{00}} \quad \text{and} \quad \bar{y} = \frac{m_{01}}{m_{00}} , \quad \mu_{pq} = \sum_x \sum_y (x - \bar{x})^p \cdot (y - \bar{y})^q f(x, y) " \tag{3}$$

Central moments change when a scaling normalization is used, as,

$$" \eta_{pq} = \mu_{pq} / \mu_{00}^y , \quad y = [(p + q) / 2] + 1 " \tag{4}$$

Specifically, Hu (1962) proposes seven values independent of object orientation, scale, and position. These values are obtained by normalizing central moments up to the third order. The seven defining moments are listed as follow [30-32]:

$$\begin{aligned}
 M1 &= (\eta_{20} + \eta_{02}) \\
 M2 &= (\eta_{20} - \eta_{02})^2 + 4\eta_{11}^2 \\
 M3 &= (\eta_{30} - 3\eta_{12})^2 + (3\eta_{21} - \eta_{03})^2 \\
 M4 &= (\eta_{30} + \eta_{12})^2 + (\eta_{21} + \eta_{03})^2 \\
 M5 &= (\eta_{30} - 3\eta_{12})(\eta_{30} + \eta_{12}) [(\eta_{30} + \eta_{12})^2 - 3(\eta_{21} + \eta_{03})^2] + (3\eta_{21} - \eta_{03})(\eta_{21} + \eta_{03}) [3(\eta_{30} + \eta_{12})^2 - (\eta_{21} + \eta_{03})^2] \\
 M6 &= (\eta_{20} - \eta_{02})[(\eta_{30} + \eta_{12})^2 - (\eta_{21} + \eta_{03})^2] + 4\eta_{11}(\eta_{30} + \eta_{12})(\eta_{21} + \eta_{03}) \\
 M7 &= (3\eta_{21} - \eta_{03})(\eta_{30} + \eta_{12}) [(\eta_{30} + \eta_{12})^2 - 3(\eta_{21} + \eta_{03})^2] - (\eta_{30} - 3\eta_{12})(\eta_{21} + \eta_{03}) [3(\eta_{30} + \eta_{12})^2 - (\eta_{21} + \eta_{03})^2]
 \end{aligned} \tag{5}$$

3.1.3.2. First-order histogram-based features

Mean, variance, skewness, and kurtosis are the first-order statistics used to describe this study's histogram-based characteristics. Let k be a random parameter representing a gray scale of an image, and p (k_i), (I = 0, 1, 2, 3, ... L-1), be the matching histogram if (L) is the total number of grayscale values [33-34]. These statistics describe the shape of the distribution [34].

1 – Mean : m

$$= \sum_{i=0}^{L-1} k_i P(k_i) \tag{6}$$

The mean provides the overall average grey level across all regions, which indicates overall intensity and not the texture present.

2 – Variance: $\mu_2(k) = \sum_{i=0}^{L-1} (k_i - m)^2 P(k_i) \tag{7}$

This statistic represents variations in grayscale intensity around the mean.

3 – Skewness: $\mu_3(k) = \sum_{i=0}^{L-1} (k_i - m)^3 P(k_i)$ (8)

One may use a statistic called skewness to quantify the disproportion of grey values around the sample mean. Negative skewness indicates a data distribution skewed to the left of the mean rather than to the right. When the skewness value is positive, the data have a rightward bias.

4 – Standard Deviation: $\mu_4 = \sigma_i$

$$\sigma_i = \left[\sum_{i=0}^{L-1} (k_i - \bar{m})^2 p(k_i) \right]^{1/2} \quad (9)$$

This feature represents the deviation (or variance) between the pixels in the input image.

3.1.3.3. Gray level co-occurrence matrix

Pixels at a distance and orientation invariant are one method to derive the second-order features. Forming the matrix cooccurrence is the first step, and identifying the characteristics as a function of the matrix is the second step. The distance (d) and orientation angle (θ) of a pixel's neighbors determine its co-occurrence value. Pixels are used as a distance measurement, and degrees as an orientation measurement. The orientation is made in 45-degree intervals from zero, 45-degree, 90-degree, and 135-degree positions. One pixel is the standard spacing between image elements. The texture characteristics specified by Haralick are retrieved from the matrix co-occurrence in the following ways [35-37]:

1 – Angular second moment:

$$f1 = \sum_i \sum_j \{P(i, j)\}^2 \quad (10)$$

2 – Contrast:

$$f2 = \sum_{n=0}^{Ng-1} n^2 \left\{ \sum_{i=1}^{Ng} \sum_{j=1}^{Ng} P(i, j) \right\} \quad (11)$$

where n, Ng: No. of different grey scales in the quantized image, and |i-j| denotes the difference of grey level between corresponding pixels.

3 – Correlation:

$$f3 = \frac{\sum_i \sum_j (i, j) P(i, j) - \mu_x \mu_y}{\sigma_x \sigma_y} \quad (12)$$

The values for the mean and standard deviation of the (r,c) are indicated by $\mu_x, \sigma_x,$ and $\mu_y, \sigma_y,$ accordingly.

4 – Sum of square:

$$f4 = \sum_i \sum_j (i - \mu)^2 P(i, j) \quad (13)$$

The matrix's average value is denoted as μ

5 – Inverse difference moment:

$$f5 = \sum_i \sum_j \frac{1}{1 + (i - j)^2} P(i, j) \quad (14)$$

6 – Sum Average:

$$f6 = \sum_{i=2}^{2Ng} iP_{x+y}(i) \quad (15)$$

Where “ $p_{x+y}(K) = \sum_{i=1}^{Ng} \sum_{j=1}^{Ng} P(i, j),$
 $k = 2, 3, \dots, 2k_g, k = i + j$ ”

7 – Sum Variance:

$$f7 = \sum_{i=2}^{2Ng} (i - f_8)^2 P_{x+y}(i) \quad (16)$$

8 – Sum Entropy:

$$f8 = - \sum_{i=2}^{2Ng} P_{x+y}(i) \log\{P_{x+y}(i)\} \quad (17)$$

9 – Entropy:

$$f9 = - \sum_i \sum_j P(i, j) \log(P(i, j)) \quad (18)$$

10 – Difference Variance:

$$f10 = \text{variance of } P_{x-y} \quad (19)$$

Where “ $p_{x-y}(K) = \sum_{i=1}^{Ng} \sum_{j=1}^{Ng} P(i, j),$
 $k = 0, 1, \dots, Ng - 1$ and $k = |i - j|$ ”

11 – Difference entropy:

$$f11 = - \sum_{i=0}^{Ng-1} P_{x-y}(i) \log \{P_{x-y}(i)\} \quad (20)$$

12 – Information measure of correlation 1:

$$f12 = \frac{HXY - HXY1}{\max\{HX, HY\}} \quad (21)$$

13 – Information measure of correlation 2:

$$f_{13} = (1 - \exp[-2.0 (HXY2 - HXY)])^{1/2} \quad (22)$$

$$"HXY = -\sum_i \sum_j P_{(i,j)} \log(P_{(i,j)})"$$

where HX and HY are entropies of p_x and p_y , and

$$"HXY1 = -\sum_i \sum_j P_{(i,j)} \log\{p_x(i)p_y(j)\}" ,$$

$$"HXY2 = -\sum_i \sum_j p_x(i)p_y(j) \log\{p_x(i)p_y(j)\}" ,$$

$$"p_x(i) = \sum_{j=1}^{N_g} P_{(i,j)}" , "p_y(j) = \sum_{i=1}^{N_g} P_{(i,j)}" \quad (23)$$

14 – Maximal Correlation Coefficients:

$$f_{14} = (\text{Second largest eigen value of } Q)^{1/2} \quad (24)$$

Where: $"Q(i, j) = \sum_k \frac{p(i,k)p(j,k)}{p_x(i)p_y(k)} \text{ and } k = 2, 3, \dots, 2k_g"$ (25)

3.1.4. Classification

When it comes to interpreting data, information, and knowledge, fuzzy logic may bridge the gap between what humans understand and what computers do. However, it cannot translate and simulate the procedure by which human intellect is transformed into rule-based, self-learning. Neuro-fuzzy systems, which are the result of combining the broad theory of artificial neural networks (ANNs) with fuzzy logic, are an effective and robust technique for real-world modeling input into smart devices [28].

3.1.4.1. ANFIS for classification

To lower the error rate, ANNs may automatically update the membership functions and interactively train the network. ANFIS is built on this principle. The ANFIS design may be considered a neural network with five layers of computation. An adaptive node is present in the first and fourth layers, whereas the other layers are all fixed, following the illustration in Fig. 3, where the circle and square represent the fixed and adaptive nodes, respectively [38-40].

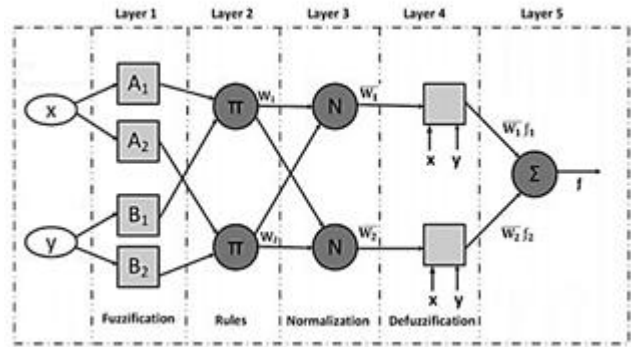


Figure. 3 ANFIS architecture [38-40]

ANFIS encourages learnability as well as flexibility in use, a fuzzy Sugeno model embedded in an adaptive systems structure. ANFIS modeling becomes more organized and less dependent on technical expertise. An ANFIS is proposed using two Sugeno fuzzy if-then rules of the 1st order [38-40]:

"R1: If (x is A_1) and (y is B_1) then $(f = p_1x + q_1y + r_1)$ " (26)

"R2: If (x is A_2) and (y is B_2) then $(f = p_2x + q_2y + r_2)$ " (27)

Inputs (x, y), Fuzzy Sets (A_i, B_i), outputs (f_i) that it inside the fuzzy area that the fuzzy rule creates, and learned design parameters (r_i, q_i, p_i). ANFIS framework is used to enforce these two guidelines.

L1: It is made up of two adaptive nodes that adjust the value of a function parameter based on the data fed into them inputs (x, y). The output of the node provides the membership level associated with the input value through:

$$\begin{cases} "O^1_i = \mu A_i(x), & i = 1, 2" \\ "O^1_i = \mu B_{i-2}(y), & i = 3, 4" \\ "\mu A_i(x), \mu B_{i-2}(y)", \end{cases} \quad (28)$$

They are entirely malleable and may be assigned any value representing fuzzy membership functions. For instance, applying a bell-shaped membership function controlled by the membership function parameters $a_i, b_i,$ and $c_i,$ as an illustration, [38-40]:

$$\mu A_i(x) = \frac{1}{1 + \left\{ \left(\frac{x-c_i}{a_i} \right)^2 \right\}^{b_i}} \quad (29)$$

L2: Similar to a node in a neural network's hidden layer, the nodes here are fixed and unable to change state. These nodes multiply the signal from the adaptive nodes before sending it on to the nodes in the subsequent layer.

The strength of the firing of the rules inherited by the adaptive nodes in the previous layer is represented by the nodes in this layer. This layer's outputs can be interpreted as [38-40]:

$$O^2_i = w_i \mu A_i(x) \mu B_i(y), \quad (30)$$

Where w_i is the production from each node and $i = 1, 2, \dots$ etc.

L3: It consists of fixed nodes. They are marked with an N to show that summation of the strengths of every rule is used to determine the firing strength of rule i . results of this layer are so normalized by the following expression [38-40]:

$$O^3_i = \bar{w}_i = \frac{w_i}{\sum_i w_i} = \frac{w_i}{w_1 + w_2}, \text{ where } i=1,2 \quad (31)$$

L4: It consists of adaptive nodes called the defuzzification layer. What happens in this layer can be thought of as how each rule affects the final result. W_i represents the layer three output. the i^{th} node's function is [38-40]:

$$O^4_i = \bar{w}_i f_i = \bar{w}_i (p_i x + q_i y + r_i) \quad (32)$$

Consequent parameters (p_i, q_i, r_i) where $i=1,2$, are the parameters that are produced by this layer.

L5: Similarly to an ANN, the last output layer contains just one "output node". At this node, the signals from the previous layer are summed. These numbers represent the fuzzy system's measurable, useful output. The error can be reduced by using this output in the training and control loops and then back-propagating the results. Consequently, the model's final results are as follows [38-40]:

$$O^5_i = \sum_i \bar{w}_i f_i = \frac{\sum_i w_i f_i}{\sum_i w_i}, \quad i=1,2 \quad (33)$$

RESULTS AND DISCUSSION

The Both the experimental dataset and the empirical examination outcomes are discussed in this section.

4.1. Dataset

The conclusions of this study are supported by data from the olive data set, which can be accessed at <https://github.com/sinanuguz/CNN>. 700 (70% training phase, 30% testing phase) of 3400 images of olive leaves were acquired in Denizli, Turkey, during spring and summer. Fig. 4 shows a sample of the Olive leaves disease dataset. The images in datasets can be divided into two categories: those showing healthy leaves and those showing leaves infested with *Aculus olearius* and the olive peacock.

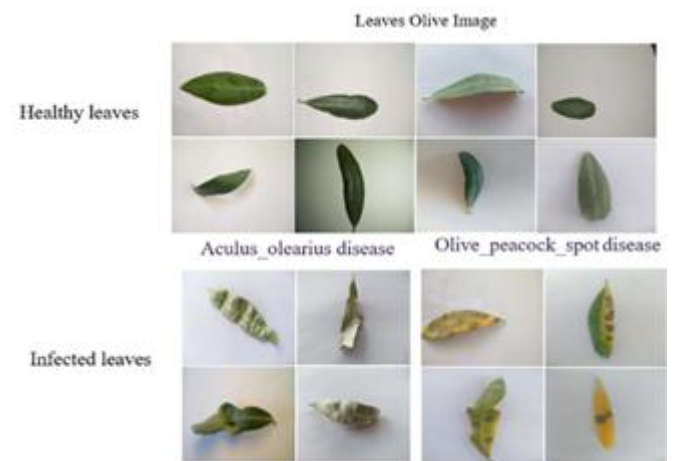


Figure. 4 Sample of Olive leaves healthy and infected

4.2. Experiments result

It is the intention of the suggested technique to employ an ANFIS based on hybrid features for olive leaf classification. Evaluation and proof of the suggested model's validity are accomplished using evolution measures such as accuracy (Ac), true positive rate (TPR), F1-score, recall (R), false positive rate (TNR), and precision(P). The suggested model's experimental results with the Histogram of Gradient (HOG) are shown in Table 1.

Model	TPR	TNR	Ac	P	R	F1
HOG+ANFIS	0.80	0.93	0.86	0.92	0.80	0.85
ANFIS	0.98	0.99	0.98	0.98	0.98	0.98

Table 1. Performance indicators for the suggested model using HOG and ANFS

Table 1 shows that the presented system and its combination achieve good results, as the accuracy reaches about 98.5%. Fig. 5 displays the relationship analysis using HOG+ANFS, which may be used to verify the accuracy of the presented system. The proposed system obtained an optimal result near the red dot from the upper left compared with HOG+ANFS. In addition, Table 2 presents the proposed method against some commonly used classification techniques.

CONCLUSION

Olive leaf recognition can be performed in an automated system using an ANFIS based on hybrid features. The K-Means method is applied to find an image's interest regions. This K-Means method gives good segmentation results. Using the ANFIS method for classification leads to higher performance results. The system presented in this work achieves (98.5%) in recognizing whether olive leaves are healthy or infected.

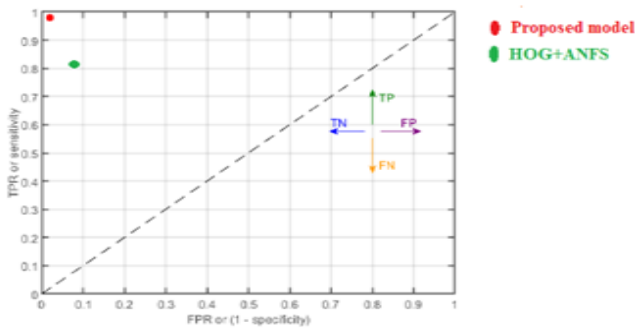


Figure. 5 The relation between TPR and FPR of the suggested model

Table 2. Comparison of the proposed model with recent works

Ref.	Dataset	Features	Classifier	Accuracy
Raouhi et al. [23]	Olive disease dataset (ODD)	-	MobileNet architecture using Rmsprop algorithms	92,59 %
Sinha et al. [24]	Healthy and spot diseases (peacock spot and neofabrea)	GLCM (Energy, Entropy, Contrast, Homogeneity)	energy and entropy	Entropy (r=0.92) and energy (r=0.97)
Uğuz et al. [18]	CNN_olive_dataset (Healthy, and Olive peacock spot, Aculus olearius diseases)	-	CNN model, Transfer learning-VGG16, VGG19 With SGD, AdaGrad, Adam, and RMS Prop optimization	88% without data augmentation 95% applied data augmentation
Alshammari et al. [19]	-	-	AlexNet-GA, DenseNet-GA and ResNet-GA	98%

Ref.	Dataset	Features	Classifier	Accuracy
Alshammari et al. [21]		Visual Feature Extraction: ViT + Visual Geometry Group (VGG)	CNN	97%
Proposed methodology		Histogram, GLCM, and Moment Invariants	ANFIS	98.5%

Acknowledgments

The authors would like to thank Mustansiriyah University (www.uomustansiriyah.edu.iq) Baghdad-Iraq for their support in the present work.

REFERENCES

- [1]. S. K. Jarallah, and S. A. Mahmood, "Query-Based Video Summarization System Based on Light Weight Deep Learning Model", *International Journal of Intelligent Engineering and Systems*, Vol. 15, No. 6, pp. 247–262, 2022, doi:10.22266/ijies2022.1231.24.
- [2]. A. M. Jalil, F. S. Hasan, and H. A. Alabbasi, "Speaker Identification Using Convolutional Neural Network for Clean and Noisy Speech Samples", In: *Proc. of First International Conference of Computer and Applied Sciences (CAS)*, Baghdad, Iraq, pp. 57-62, 2019, doi:10.1109/CAS47993.2019.9075461.
- [3]. A. S. Mahdi and S. A. Mahmood, "An Edge Computing Environment for Early Wildfire Detection", *Annals of Emerging Technologies in Computing (AETiC)*, Vol. 6, No. 3, pp. 56-68, 2022, doi:10.33166/AETiC.2022.03.005.
- [4]. A. S. Mahdi, and S. A. Mahmood, "Wildfire Detection System using Yolov5 Deep Learning Model", *International Journal of Computing and Digital Systems*, Vol. 14, No. 1, pp. 10149-10158, 2023, doi:10.12785/ijcds/140188.
- [5]. H. K. Hoomod and Z. S. Amory, "Temperature Prediction Using Recurrent Neural Network for Internet of Things Room Controlling Application", In: *Proc. of the 2020 5th International Conf. on Communication and Electronics Systems (ICCES)*, Coimbatore, India, pp. 973-978, 2020, doi:10.1109/ICCES48766.2020.9137885.
- [6]. O. A. Alawi, H. M. Kamar, S. Q. Salih, S. I. Abba, W. Ahmed, R. Z. Homod, ... Z. M. Yaseen, "Development of optimized machine learning models for predicting flat plate solar collectors thermal efficiency associated with Al2O3-water nanofluids", *Engineering Applications of Artificial Intelligence*, Vol. 133, Part B, No. 108158, 2024, doi:10.1016/j.engappai.2024.108158.
- [7]. Z. H. Ali, H. M. Salman, and A. H. Harif, "SMS Spam Detection Using Multiple Linear Regression and Extreme Learning Machines", *Iraqi Journal of science*, Vol. 64, No. 10, pp. 5442-5451, 2023, doi: 10.24996/ijcs.2023.64.10.45.
- [8]. S. A. Mahmood, A. M. Abid, and W. A. K. Naser, "Contextual Anomaly Detection Based Video Surveillance System", In: *Proc. of 2021 11th IEEE International Conf. on Control System, Computing and Engineering (ICCSCE)*, Penang, Malaysia, pp.120-125, 2021, doi:10.1109/ICCSCE52189.2021.9530859.
- [9]. M. H. Abdalla, J. Majidpour, R. A. Rasul, A. A. Alsewari, T. A. Rashid, A. M. Ahmed, ..., S. Q. Salih, "Sentiment Analysis Based on Hybrid Neural Network Techniques Using Binary

- Coordinate Ascent Algorithm”, in IEEE Access, Vol. 11, No. 108158, pp. 134087 - 134099, 2023, doi: 10.1109/ACCESS.2023.3334980.
- [10]. S. H. Jasim, R. A. Haleot, and S. A. Thajeel, “Brain Stroke Segmentation Based on U-NET Algorithm”, In: Proc. of the 2022 International Conf. on Data Science and Intelligent Computing (ICDSIC), pp. 208-211, 2022, doi:10.1109/ICDSIC56987.2022.10076085.
- [11]. M. S. Jabber, “Documents Image Classification and Retrieval Based on Logo Recognition”, Iraqi Journal of Information Technology, Vol. 8, No. 1, pp. 59-73, 2017.
- [12]. S. A. Patel and P. A. Barot, “Parallel Custom Deep Learning Model for Classification of Plant Leaf Disease Using Fusion of Features”, International Journal of Intelligent Engineering and Systems, Vol. 17, No. 2, pp. 50–60, 2024, doi:10.22266/ijies2024.0430.05.
- [13]. M. Tiwari, H. Kumar, N. Prakash, S. Kumar, R. Neware, S. Tripathi, and R. Agarwal, “Tomato Disease Detection Using Vision Transformer with Residual L1-Norm Attention and Deep Neural Networks”, International Journal of Intelligent Engineering and Systems, Vol. 17, No. 1, pp. 679–688, 2024, doi:10.22266/ijies2024.0229.57.
- [14]. H. Darmawan, M. Yuliana, and M. Z. S. Hadi, “Cloud-based Paddy Plant Pest and Disease Identification using Enhanced Deep Metric Learning and k-NN Classification with Augmented Latent Fusion”, International Journal of Intelligent Engineering and Systems, Vol. 16, No. 6, pp. 158–170, 2023, doi:10.22266/ijies2023.1231.14.
- [15]. A. Ksibi, M. Ayadi, B. O. Soufiene, M. M. Jamjoom, and Z. Ullah, “MobiRes-Net: A Hybrid Deep Learning Model for Detecting and Classifying Olive Leaf Diseases”, Applied Sciences, Vol. 12, No. 20, p. 1-19, 2022, doi:10.3390/app122010278.
- [16]. I. Navrozidis, T. Alexandridis, D. Moshou, A. Haugomard, and A. Lagopodi, “Implementing Sentinel-2 Data and Machine Learning to Detect Plant Stress in Olive Groves”, Remote Sensing, Vol. 14, No. 23, p. 1-22, 2022, doi:10.3390/rs14235947.
- [17]. A. Sanaeifar, C. Yang, M. de la Guardia, W. Zhang, X. Li, and Y. He, “Proximal hyperspectral sensing of abiotic stresses in plants”, Science of The Total Environment, Vol. 861, No. 160652, 2023, doi:10.1016/j.scitotenv.2022.160652.
- [18]. S. Uğuz, and N. Uysal, “Classification of Olive Leaf Diseases Using Deep Convolutional Neural Networks”, Neural Computing and Applications, Vol. 33, No. 5, pp. 4133–4149, 2021, doi:10.1007/s00521-020-05235-5.
- [19]. H. Alshammari, K. Gasmi, M. Krichen, L. B. Ammar, M.O. Abdelhadi, A. Boukrara, and M. A. Mahmood, “Optimal Deep Learning Model for Olive Disease Diagnosis Based on An Adaptive Genetic Algorithm”, Wireless Communications and Mobile Computing, Vol. 2022, pp.1- 13, 2022, doi:10.1155/2022/8531213.
- [20]. V. Meshram, K. Patil, V. Meshram, D. Hanchate, and S. D. Ramkteke, “Machine learning in agriculture domain: A state-of-art survey”, Artificial Intelligence in the Life Sciences, Vol. 1, p. 1-11, 2021, doi:10.1016/j.aailsci.2021.100010.
- [21]. H. Alshammari, K. Gasmi, I. B. Ltaifa, M. Krichen, L. B. Ammar, and M. A. Mahmood, “Olive Disease Classification Based on Vision Transformer and CNN Models”, Computational Intelligence and Neuroscience, Vol. 2022, pp.1-10, 2022, doi:10.1155/2022/3998193.
- [22]. A. Abbas, and S. Deny, “Progress and limitations of deep networks to recognize objects in unusual poses”, In: Proc. of The Thirty-Seventh AAAI Conference on Artificial

- Intelligence (AAAI-23), pp. 160–168, 2022, doi:10.48550/arXiv.2207.08034.
- [23]. E. Raouhi, M. Lachgar, H. Hrimech, and A. Kartit, “Optimization Techniques in Deep Convolutional Neuronal Networks Applied to Olive Diseases Classification”, *Artificial Intelligence in Agriculture*, Vol. 6, pp. 77-89, 2022, doi:10.1016/j.aiia.2022.06.001.
- [24]. A. Sinha, and R. S. Shekhawat, “Olive Spot Disease Detection and Classification Using Analysis of Leaf Image Textures”, *Procedia Computer Science*, Vol. 167, pp. 2328–2336, 2020, doi:10.1016/j.procs.2020.03.285.
- [25]. M. Anand and M. Sundaram, “Channel and Spatial Attention Aware UNet Architecture for Segmentation of Blood Vessels, Exudates and Microaneurysms in Diabetic Retinopathy”, *International Journal of Intelligent Engineering and Systems*, Vol. 17, No. 2, pp. 1–16, 2024, doi:10.22266/ijies2024.0430.01.
- [26]. G. Bompem, D. Pandluri, “Batch Normalization Based Convolutional Neural Network for Segmentation and Classification of Brain Tumor MRI Images”, *International Journal of Intelligent Engineering and Systems*, Vol. 17, No. 2, pp. 39–49, 2024, doi:10.22266/ijies2024.0430.04.
- [27]. M. Waleed, T.W. Um, A. Khan, and U. Khan, “Automatic Detection System of Olive Trees using Improved K-Means Algorithm”, *Remote Sensing*, Vol. 12, No. 5:760, pp. 1–16, 2020, doi:10.3390/rs12050760.
- [28]. K. Shao, G. Mei, and Y. Wu, “Investigating Changes in Global Distribution of Ozone in 2018 Using K-Means Clustering Algorithm”, *Journal of Computational Mathematics and Data Science*, Vol. 3, pp.1-14, 2022, doi:10.1016/j.jcmds.2022.100028.
- [29]. A. Yousuf and U. Khan, “Ensemble Classifier for Plant Disease Detection”, *International Journal of Computer Science and Mobile Computing*, Vol. 10, No.1, pp. 14-22, 2021, doi:10.47760/ijcsmc.2021.v10i01.003.
- [30]. Z. Wu, S. Jiang, X. Zhou, Y. Wang, Y. Zuo, Z. Wu, ... Q. Liu,” Application of Image Retrieval Based on Convolutional Neural Networks and Hu Invariant Moment Algorithm in Computer Telecommunications,” *Computer Communications*, Vol. 150, pp.729–738, 2020, doi:10.1016/j.comcom.2019.11.053.
- [31]. R. Hidayat, A. Harjoko, and A. Musdholifah, “A Robust Image Retrieval Method Using Multi-Hierarchical Agglomerative Clustering and Davis-Bouldin Index”, *International Journal of Intelligent Engineering and Systems*, Vol. 15, No. 2, pp. 441– 453, 2022, doi:10.22266/ijies2022.0430.40.
- [32]. H. Mo, H. Hao, and H. Li, “Geometric Moment Invariants to Spatial Transform and N-Fold Symmetric Blur”, *Pattern Recognition*, Vol. 115, 2021, doi:10.1016/j.patcog.2021.107887.
- [33]. A. Daoui, H. Karmouni, M. Sayyouri, H. Qjidaa, M. Maaroufi, and B. Alami,” New Robust Method for Image Copyright Protection Using Histogram Features and Sine Cosine Algorithm”, *Expert Systems with Applications*, Vol. 177, pp.1-18, Sep. 2021, doi:10.1016/j.eswa.2021.114978.
- [34]. K. Djunaidi, H. B. Agtriadi, D. Kuswardani, and Y. S. Purwanto, “Gray Level Co-occurrence Matrix Feature Extraction and Histogram in Breast Cancer Classification with Ultrasonographic Imagery”, *Indonesian Journal of Electrical Engineering and Computer Science*, Vol. 22, No. 2, May 2021, pp. 795-800, doi:10.11591/ijeecs.v22.i2.pp795-800.
- [35]. R. M. Haralick, K. Shanmugam, and I. Dinstein,” Textural Features for Image Classification”, in *IEEE Transactions on Systems, Man, and Cybernetics*, Vol. SMC-3, No. 6, pp. 610-621, 1973, doi:10.1109/TSMC.1973.4309314.

- [36]. S. A. Alazawi, N. M. Shati, and A. H. Abbas,” Texture Features Extraction Based on GLCM for Face Retrieval System”, *Period. Eng. Nat. Sci.*, Vol. 7, No. 3, pp. 1459–1467, 2019, doi:10.21533/pen.v7i3.787.
- [37]. A. Ramola, A. K. Shakya, and D. V. Pham,” Study of Statistical Methods for Texture Analysis and Their Modern Evolutions”, *Eng. Reports*, Vol. 2, No. 4: e12149, pp. 1–24, 2020, doi:10.1002/eng2.12149.
- [38]. C. Qi, H.-B. Ly, L. M. Le, X. Yang, L. Guo, and B. T. Pham,” Improved Strength Prediction of Cemented Paste Backfill Using a Novel Model Based on Adaptive Neuro Fuzzy Inference System and Artificial Bee Colony”, *Construction and Building Materials*, Vol. 284, pp. 1-14, 2021, doi:10.1016/j.conbuildmat.2021.122857.
- [39]. A. Tay, F. Lafont, and J.-F. Balmat,” Forecasting Pest Risk Level in Roses Greenhouse: Adaptive Neuro-Fuzzy Inference System vs Artificial Neural Networks”, *Information Processing in Agriculture*, Vol. 8, No. 3, pp. 386-397, 2021, doi:10.1016/j.inpa.2020.10.005.
- [40]. İ. Güler, and E. D. Übeyli,” Adaptive Neuro-Fuzzy Inference System for Classification of EEG Signals Using Wavelet Coefficients”, *Journal of Neuroscience Methods*, Vol. 148, No. 2, pp. 113–121, 2005, doi:10.1016/j.jneumeth.2005.04.013.